RESEARCH ARTICLE | SEPTEMBER 23 2014

The jet in crossflow

Ann R. Karagozian

Physics of Fluids 26, 101303 (2014)
https://doi.org/10.1063/1.4895900

PHYSICS OF FLUIDS **26**, 101303 (2014)

The jet in crossflow

Ann R. Karagozian[a),b)]
Mechanical and Aerospace Engineering Department, University of California, Los Angeles, California 90095, USA

(Received 27 June 2014; accepted 2 September 2014; published online 23 September 2014; publisher error corrected 31 March 2015)

The jet in crossflow, or transverse jet, is a flowfield that has relevance to a wide range of energy and propulsion systems. Over the years, our group's studies on this canonical flowfield have focused on the dynamics of the vorticity associated with equidensity and variable density jets in crossflow, including the stability characteristics of the jet's upstream shear layer, as a means of explaining jet response to altered types of excitation. The jet's upstream shear layer is demonstrated to exhibit convectively unstable behavior at high jet-to-crossflow momentum flux ratios, transitioning to absolutely unstable behavior at low momentum flux and/or density ratios, with attendant differences in shear layer vorticity evolution and rollup. These differences in stability characteristics are shown to have a significant effect on how one optimally employs external excitation to control jet penetration and spread, depending on the flow regime and specific engineering application. Yet recent unexpected observations on altered transverse jet structure under different flow conditions introduce a host of unanswered questions, primarily but not exclusively associated with the nature of molecular mixing, that make this canonical flowfield one that is of great interest for more extensive exploration. © *2014 AIP Publishing LLC*. [http://dx.doi.org/10.1063/1.4895900]

I. INTRODUCTION AND BACKGROUND

Jets injected perpendicularly into a cross-stream can be found in a range of technological systems.[1,2] The jet in crossflow (JICF) or transverse jet is utilized in dilution or primary air jet injection in gas turbine combustors, to accomplish mixture ratio and NOx control as well as turbine hot section cooling; in film cooling of turbine blades; in primary fuel injection in high speed air-breathing engines; and in thrust vector control for missiles and other high speed vehicles. Transverse jets are also found in environmental control systems, including control of effluent from chimney and smokestack plumes as well as liquid effluent dispersal in streams. Hence many variations on this canonical flowfield exist,[2] including gas injection into gas; liquid injection into a crossflow of liquid or gas; reactive fuel jets injected into a cross-stream of oxidizer; jet fluid injection that is either elevated or flush with respect to a surface; circular or rectangular jets of various aspect ratios; and gas or liquid injection into high speed crossflows of air, with bow shocks or other wave structures influencing jet behavior. The range of flow conditions and applications of the transverse jet requires a thorough understanding of the structural, mixing, and, when relevant, reactive flow characteristics in order to determine optimum operating conditions and control strategies.

The interaction of the jet and crossflow creates a complex set of flow structures and vortex systems, as shown for the round transverse jet with flush perpendicular injection in Figure 1. The counter-rotating vortex pair (CVP) structure observed to dominate the jet cross-section[3,4] is generated in the nearfield region of the jet and is thought to be associated with the evolution of vorticity in the jet's shear layer[5–8] as well as pressure differences between the upstream and downstream regions of the jet.[9,10] In addition to the CVP, horseshoe vortices are observed to wrap around the jet column[11]

[a)] Author presented this paper as an invited talk at the 66th Annual Meeting of the APS Division of Fluid Dynamics, 24–26 November 2013, Pittsburgh, Pennsylvania, USA.

[b)] ark@seas.ucla.edu

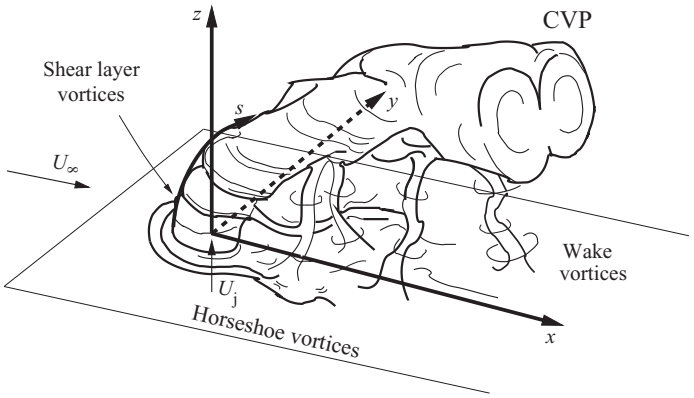

FIG. 1. Schematic of the transverse jet, introduced flush with respect to the injection wall, including relevant vortical structures and orientation of coordinate axes. Shown are the counter-rotating vortex pair (CVP) as well as the jet's upstream shear layer vortices, wake vortices, and horseshoe vortex structures. Adapted with permission from T. F. Fric and A. Roshko, J. Fluid Mech. **279**, 1–47 (1994). Copyright 1994 by Cambridge University Press.

and can become unsteady at specific flow conditions.[12] Wake vortices forming on the lee side of the flush-injected JICF are another prominent flow feature and have been determined to contain wall boundary layer fluid which is drawn into the jet.[13] All of these vortical features play a role in the transverse jet's structure and mixing characteristics.[14]

Among the important non-dimensional parameters associated with the transverse jet include the jet-to-crossflow velocity ratio, $R \equiv U_j/U_\infty$, the jet-to-crossflow density ratio, $S \equiv \rho_j/\rho_\infty$, the jet-to-crossflow momentum flux ratio, $J \equiv SR^2$, and the jet Reynolds number, $Re_j \equiv U_j D/\nu_j$, which is based on the jet exit diameter D and, most commonly, the bulk or mean jet velocity, U_j. Typical flow and operating conditions can vary quite widely for the JICF, depending on the specific application, even in the subsonic regime. For example, for applications involving dilution air jets and thrust vector control, the degree of jet penetration as well as molecular mixing of the jet with surroundings is generally desired to be high. Since mixing and penetration have been correlated with each other for a range of JICF geometries,[15] the momentum flux ratio J for these applications tends to exceed 25, and often involves $J > 100$. In contrast, film cooling to enable thermal protection of turbine blades involves arrays of jets injected perpendicularly from the blade surface into hot crossflow at relatively low momentum flux ratios, often $J < 5$ or even $J < 1$, to enable the jets to adhere to the surface of the blades while cooling them, rather than penetrating deeply into the hot crossflow.[16,17] Yet turbine blade film cooling jets can be subject to separation occurring over the trailing portion of the suction surface, and this is especially problematic at lower Reynolds numbers that are present in classes of small gas turbine engines typically used or planned for use in high-altitude air vehicles. In fact, many of the features of the transverse jet, even those shown notionally in Fig. 1, are dependent on the particular flow regime in terms of momentum flux ratio, Reynolds number, and density ratio, as well as specific injection geometry, as described below. Hence it has been of interest over several decades to be able to understand, predict, and control features of the jet in crossflow across a wide range of flow conditions.

A. Transverse jet vorticity generation and evolution

Many of the global features of the transverse jet can be understood and, to a limited extent, predicted on the basis of the dynamics of the CVP. The generation and evolution of these vortical structures has been a matter of some debate and examination over the past several decades. Broadwell and Breidenthal[18] suggest that the CVP fundamentally arises from the impulse associated with the jet and thus is a global feature of the far field, in which the CVP is convected downstream by the crossflow. This concept, coupled with a simple nearfield model for the deflection of crossflow about the jet, enables vorticity-based, low-order models for the transverse jet to

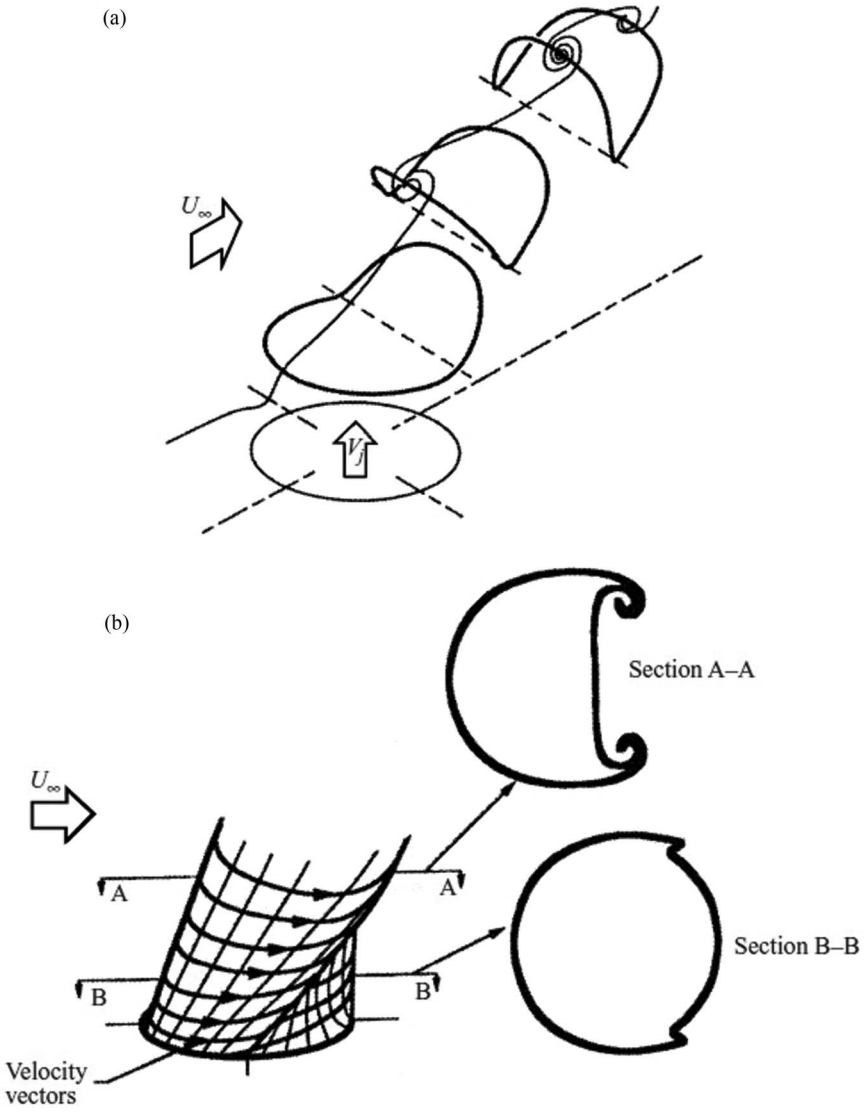

FIG. 2. Interpretation of transverse jet shear layer evolution by Kelso, Lim, and Perry,[7] including (a) isometric view of the tilting of shear layer vortex rings and (b) reorientation of the shear layer vorticity, leading to folding of the vortex sheet and eventual formation of the CVP. Reprinted with permission from R. M. Kelso, T. T. Lim, and A. E. Perry, J. Fluid Mech. **306**, 111–144 (1996). Copyright 1996 by Cambridge University Press.

predict global trajectories and flame lengths reasonably well[19,20] at higher jet-to-crossflow velocity ratios ($R \geq 4$).

Detailed experimental studies in the nearfield of the JICF have suggested that the CVP is formed by the vortex sheet emanating from the jet nozzle or pipe.[5–7,13] The experiments of Kelso, Lim, and Perry[7] in both water and air suggest that periodic vortex ring rollup from the nozzle occurs for the round jet injected flush into crossflow, similar to that which occurs in the free jet, yet superposed on this process is a re-orientation of this shear layer vorticity that is imposed by the crossflow, which leads to a folding of the cylindrical vortex sheet. The superposition of these two mechanisms is thought to result in a tilting of the upstream portion of the ring oriented with the mean curvature of the jet, and a tilting and folding of the downstream portion of the ring aligned with the direction of the jet. It is this tilting and folding which is thought to contribute to the circulation of the CVP, shown notionally in Fig. 2. Kelso, Lim, and Perry[7] state that "the shear layer of the jet folds and rolls up very near to the pipe exit, leading to or contributing to the formation of the CVP," as suggested in the figure.

The relationship of the CVP to transverse jet mixing characteristics has also been of great interest over many decades.[3,4] Among the benefits of using the jet in crossflow in many practical environments is the enhancement of the entrainment of crossflow into the vicinity of the jet and the associated enhancement of the molecular mixing of the two fluids. Entrainment by a subsonic transverse jet or flame is typically seen to be much greater than that by a free jet or a buoyant turbulent jet.[14,18,20,21] For transverse jets in high speed airbreathing applications, e.g., for fuel injection into high speed crossflow, the degree of penetration of the jet is of particular importance.[22–24] Rapid fuel penetration, mixing with crossflow, and ignition and sustainment of combustion processes are highly desirable, since high air speeds entering the combustion chamber (supersonic in the case of a scramjet) require very rapid completion of the reaction process.[25] With respect to the relationship between the CVP and mixing enhancement, Smith and Mungal[14] suggest that, in light of the evolving development of the CVP in the nearfield of the jet, the enhanced mixing in the jet's nearfield corresponds to and likely results from the structural formation of the CVP rather than its fully developed existence. Hence at many levels, the nature of the CVP and its initiation are important features of the transverse jet.

B. Temporally forced jets in crossflow

Among the means by which control of transverse jets has been studied in recent years involves temporal excitation of the jet fluid. Through such active excitation, control of vorticity generation may be accomplished. Fundamental experiments on pulsed or acoustically driven transverse jets[7,26–31] suggest that, for certain excitation conditions, increased jet penetration into the crossflow and/or increased spread and mixing may be achieved. Yet specific conditions yielding significant jet response to forcing vary rather widely among these different sets of experiments, which have been conducted in both liquids[27,28] and gases.[26,29–31]

Some of these recent studies have focused on sinusoidal or sinusoidal-like excitation[7,26,30] and find improvement in transverse jet mixing when forcing is applied at specific values of the Strouhal number (based on forcing frequency f_f, mean jet velocity, and jet orifice diameter, $St_f \equiv f_f D/U_j$). In some cases, e.g., in the gas phase experiments in Narayanan, Barooah, and Cohen,[30] the forcing frequency f_f for maximized jet spread and mixing is equal to or greater than that associated with the unforced transverse jet's shear layer instability, f_o; in these experiments, the mean jet-to-crossflow velocity ratio R is fixed at 6. Significant jet response is achieved even when sinusoidal jet forcing, with a moderate peak-to-peak velocity excitation amplitude of about 30% of the mean jet exit velocity, is employed. Enhancements of 30%–46% in time-averaged entrainment, relative to that for the unforced jet, are quantified via Mie scattering-based flow visualization,[30] and the observed vorticity dynamics are similar to those predicted in Direct Numerical Simulations (DNS) of a transverse jet operating at the same flow conditions by Muldoon and Acharya.[32]

Yet sinusoidal excitation of the transverse jet does not always produce such a response. Early experimental research on controlled transverse jets at UCLA[29,31,33] focuses on acoustically forced, flush round jets in crossflow with relatively low jet-to-crossflow velocity ratios, $R = 2.56$ and 4.0, where the jet exit velocity is based on the measured centerline value. In contrast to the above-noted observations[30] at $R = 6$, experiments with forced sinusoidal excitation of the jet at $R = 2.56$ in M'Closkey *et al.*,[29] for example, show relatively little visual influence of forcing on jet behavior as compared with unforced jet behavior. Even with very large amplitude excitation, exceeding 75% of the mean jet velocity, and irrespective of the frequency of excitation, there is relatively little observed response of the transverse jet to temporal sine wave forcing.

On the other hand, M'Closkey *et al.*[29] and Shapiro *et al.*[31] show that square-wave excitation of the jet at subharmonics of the fundamental (unforced) shear layer frequency, and with the same RMS of the velocity excitation as in sinusoidal forcing, yields significant increases in the jet penetration and spread. Feedforward or open loop control is employed to enable relatively precise temporal square wave excitation of the jet fluid.[29] Comparisons of jet response to these alternative modes of excitation, imaged via smoke visualization, are shown, for example, in Fig. 3. Distinct, deeply penetrating vortical structures are formed periodically in response to square-wave forcing, creating much greater overall jet penetration and, for the relatively low duty cycle shown, a bifurcated jet

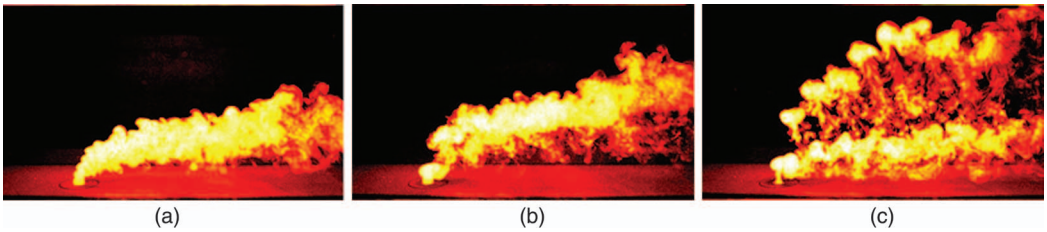

FIG. 3. Smoke visualization of the jet injected from a flush nozzle into crossflow at an average jet-to-crossflow velocity ratio of $R = 2.58$, where $U_j = 3.1$m/s and $U_\infty = 1.2$m/s. Results are shown for (a) the "unforced" jet, with an initial shear layer instability occurring at 220 Hz, (b) the jet forced with sine wave excitation at one-third the natural frequency, 73.5 Hz, and (c) the jet forced with square wave excitation at 73.5 Hz and a duty cycle of 22%. For the forced conditions, a RMS amplitude of the velocity perturbations is matched between (b) and (c) at 1.7m/s. Reprinted with permission from R. T. M'Closkey, J. King, L. Cortelezzi, and A. R. Karagozian, J. Fluid Mech. **452**, 325–335 (2002). Copyright 2002 by Cambridge University Press.

structure; this contrasts the relatively minimal response seen when the transverse jet is forced with a sinusoidal excitation with the same RMS of the velocity disturbance, also shown in this figure.

The conditions (forcing frequencies, duty cycles for square-wave excitation, amplitudes of excitation) leading to enhancement of jet penetration and spread indicate that specific values of the temporal pulse width τ can provide optimal merger and penetration of vortical structures.[31] The time scales associated with this optimization appear to be nominally related to a "universal time scale" or non-dimensional stroke ratio L/D associated with coherent vortex ring formation,[34] which is observed to be optimized for L/D in the range 3.6–4.5, where stroke length L is related to the velocity amplitude of square wave excitation, integrated over time. These observations for the transverse jet are also consistent with the ideas of Johari,[35] who suggests that transverse jet forcing with low duty cycles ($\alpha \equiv \tau/T \sim 0.2$) can lead to deeply penetrating transverse jets with distinct vortex rings. Experiments by Shapiro *et al.*[31] as well as DNS by Sau and Mahesh[36] of the transverse jet exposed to square wave-like excitation (i.e., with imperfect but approximate square waves) suggest that, as long as the temporal waveform has a sharp upsweep for the delivery of sharp pulses of vorticity, and a relatively sharp downsweep to more clearly define the pulsewidth, imperfections in the waveform have very little effect on transverse jet behavior, and that such forcing can have a profound influence on jet behavior.

It is noted that temporal square wave forcing has also been found to benefit transverse jet heat transfer processes in film cooling applications, i.e., at very low jet-to-crossflow momentum flux ratios, where enhanced jet penetration is not desirable. Pulsed transverse or "vortex generator" jets are observed[16,17] to improve cooling effectiveness at lower heat transfer coefficients, to reduce blade suction surface boundary layer separation at low Reynolds numbers, and to require an order of magnitude reduction in mean mass flow as compared with steady injection.

II. TRANSVERSE JET INSTABILITIES

A. Shear layer instabilities for equidensity and low density jets in crossflow

The difference between transverse jet response to sinusoidal excitation and to prescribed square wave excitation shown in Fig. 3 is quite striking, suggesting the importance of controlling nearfield vorticity generation in order to influence overall jet behavior. But it has also been of interest to understand why, even with such large scale jet excitation as in Fig. 3(b), jet response to sinusoidal excitation is rather minimal, in contrast to the observations of others such as Narayanan, Barooah, and Cohen,[30] for example. Recent explorations of the transverse jet's shear layer instabilities have been pursued in part to explain the reasons for these differences in jet response.

Extensive experimental explorations of the instabilities associated with the equidensity ($S = 1$) transverse jet's nearfield upstream shear layer[37,38] as well as the shear layer for the low density ($S < 1$) jet in crossflow[39] have been pursued by our group. Flow conditions in the range $1 < R < \infty$ for the equidensity jet in crossflow, and in the range $2 \leq J \leq 41$ for the low density jet in crossflow

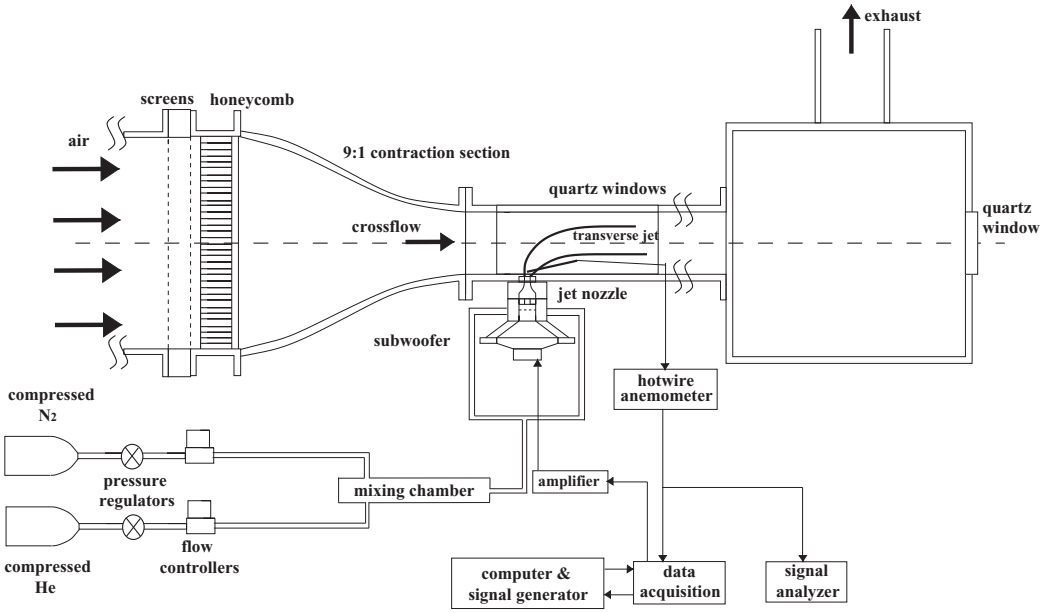

FIG. 4. Variable density transverse jet wind tunnel, and associated data acquisition and jet excitation apparatus. One additional tunnel section, of identical dimensions, was situated downstream of the test section shown. Reprinted with permission from D. R. Getsinger, C. Hendrickson, and A. R. Karagozian, Exp. Fluids **53**, 783–801 (2012). Copyright 2012 by Springer-Verlag.

(with density ratios $0.25 \leq S \leq 1.0$) have been explored, for jet Reynolds numbers in the range $1800 \leq Re_j \leq 3000$. These detailed measurements indicate significant differences in the nature of upstream shear layer instabilities for the JICF, depending on the flow regime.

The low speed wind tunnel used for low density and equidensity transverse jet shear layer experiments is shown in Fig. 4. Jet fluid is introduced through an injector situated at the bottom wall of the wind tunnel test section, issuing at room temperature into a crossflow of air. The tunnel test section is 12 cm × 12 cm in cross-section and 30 cm in length, with optical access windows (quartz) fitted to the sides and top surfaces. Alternative jet nozzles, each with a fifth-order polynomial shape, an exit diameter of 4 mm, and producing a nearly top-hat velocity profile at the exit plane in the absence of crossflow, have been explored in these studies.[37] The exit plane of one nozzle is situated flush with respect to the tunnel wall and that of the other nozzle is extended by nearly four diameters from the tunnel wall, allowing gas injection outside of the wall boundary layer created by crossflow. Flush nozzles alone are studied in greater detail in later equidensity shear layer stability studies[38] and in low density JICF studies.[39] In general, the jet fluid is composed of varying proportions of nitrogen and helium to achieve the desired jet-to-crossflow density ratio. In these transverse jet shear layer studies, spectral measurements corresponding to fluctuations in the vertical velocity (z-component) are obtained using a single-component, boundary-layer type hotwire probe. The range of Reynolds numbers and momentum flux ratios J in these studies are such that, even at low jet-to-crossflow density ratios S, buoyancy effects are not important until at least 20 diameters downstream of injection, per approximate Richardson number scaling for low density jets.[40] Further details on the tunnel, injection system, and measurement procedures may be found in Megerian *et al.*,[37] Davitian *et al.*,[38] and Getsinger, Hendrickson, and Karagozian.[39]

When the crossflow is successively increased for a fixed jet Reynolds number and fixed density ratio S in these experiments, the reduction in jet-to-crossflow velocity ratio R or momentum flux ratio J is observed to create significant alterations in the shear layer instabilities at the upstream side of the jet. For the equidensity jet in crossflow, for example, as R or J is reduced from infinity, the shear layer instabilities are observed to be strengthened, to be initiated closer to the jet orifice, and to show evidence of successively weakening subharmonic instabilities. Sample results for the transition in the nature of the shear layer spectra for equidensity flush nozzle conditions are shown in

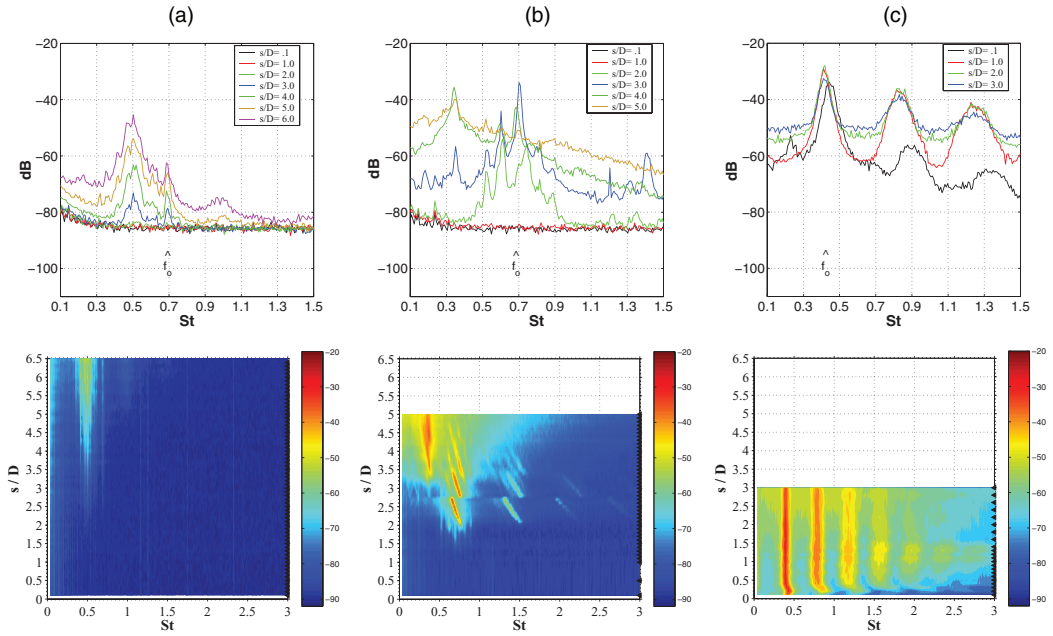

FIG. 5. Shear layer instabilities for equidensity jets ($S = 1.0$) emanating from a flush nozzle at fixed $Re_j = 2000$ (based on centerline jet velocity at the exit plane[37]). Upper images: power spectra from hotwire response at various *s/D* locations along the jet's upstream shear layer; lower images: spectra with a finer spatial grid represented by spectral magnitude contours, with the magnitude colorbar (in dB) matched for each condition. Data are shown for (a) equidensity free jet ($R \to \infty$), (b) velocity ratio $R = 6.4$, and (c) $R = 1.15$, with initial oscillation frequency given in terms of Strouhal number *St*. Reprinted with permission from S. Megerian, J. Davitian, L. S. de B. Alves, and A. R. Karagozian, J. Fluid Mech. **593**, 93–129 (207). Copyright 2007 by Cambridge University Press.

Fig. 5 for velocity ratios corresponding to the free jet ($R \to \infty$), the transverse jet at a relative high velocity ratio ($R = 6.4$), and the transverse jet at a velocity ratio below that at which a transition in spectral characteristics is observed ($R = 1.15$), for a jet Reynolds number of 2000. Note that in these earlier studies,[37,38] Re_j and R are based on the jet's centerline velocity at the exit plane rather than the mean velocity, the former being approximately 20% higher than the latter for the range of flow conditions explored. Shown in the upper row of Fig. 5 are power spectra measured by the hotwire on a course spatial grid, with each line color representing a different *s/D* location. Spectral data for a finer spatial grid represented by spectral magnitude contours, with the magnitude colorbar (in dB) matched for each condition, are shown in the lower row of this figure. Strouhal number $St \equiv f_o D/U_j$ is based on the frequency f_o of the initial instability detected along the shear layer.

As is typically observed for the free jet,[41,42] the early-developing shear-layer mode in Fig. 5(a) evolves along the layer to be taken over eventually by the "preferred mode" occurring further downstream. As R is reduced to 6.4 via increasing the crossflow velocity magnitude, U_∞, at a fixed jet Reynolds number, the instabilities are initiated closer to the jet exit, while the transverse jet's fundamental mode (as well as its higher harmonics) exhibits shifting to lower frequencies and subsequent hopping to higher frequencies in multiple stages, before eventually being reduced in magnitude farther downstream, where the subharmonic becomes dominant. Such frequency shifting/hopping behavior is a result of a shear layer tonal phenomenon, observed in both planar and axisymmetric free jets by Hussain and Zaman.[43] The presence of the hotwire probe itself influences the transverse jet shear layer, resulting in feedback that serves to alter the shear layer's fundamental instability frequency in a manner that is dependent on the distance between the probe and the jet exit. The impact of the shear layer tonal interactions with the hotwire is significantly reduced as R is lowered, however. Such tonal interactions are not observed in our experiments for the free jet (either equidensity or low density), but are determined to occur for transverse jets emanating from a flush circular nozzle, as in Fig. 5, for a range of conditions where $R > 3.1$. Thus the spectral

characteristics represented in Fig. 5(b) can be used as a spectral signature for the transverse jet at relatively high velocity ratios. As the crossflow velocity is increased for this equidensity case, however, so that R is reduced below around 3.1, the oscillations are altered quite strikingly. The fundamental shear layer mode continues to be initiated ever closer to the jet orifice with decreasing R, but exhibits the same dominant, pure tone instability throughout the shear layer. An example of the spectral characteristics for these "low" velocity or momentum flux ratios is shown in Fig. 5(c) for $R = 1.15$. The frequency-shifting behavior is altogether eliminated below approximately $R = 3.1$, and subharmonics are significantly weakened, suggesting a reduction in vortex merger and pairing at lower R values. A similar transition in spectral characteristics is observed for the transverse jet produced by the elevated nozzle,[37] but at a lower velocity ratio, $R \approx 1.2$ based on jet centerline velocity. This difference in the critical value of R is found to result from the vertical coflow along the upstream edge of the elevated nozzle that increases in magnitude with increasing crossflow velocity U_∞; coflow is known to stabilize a jet's shear layer, as documented for purely coflowing jets.[44] Once the transverse jet emanating from the elevated nozzle has been turned sufficiently at low R, however, the spectral character becomes very similar to that for the jet emanating from the flush nozzle, as indicated in Fig. 5(c).

This significantly altered behavior in the transverse jet as R is reduced below a critical value is consistent with transition in the upstream shear-layer from being convectively unstable to becoming self-sustained or absolutely unstable. The presence of global instability in a number of different types of shear flows is well known.[45] Such flows include low density axisymmetric jets in quiescent surroundings below a critical jet-to-surroundings density ratio,[40,46] countercurrent mixing layers above a critical velocity difference,[47,48] and wake flows above a critical Reynolds number.[49,50] The evidence for such a transition in the JICF shear layer includes phenomena that are extensively documented for the equidensity transverse jet[37,38] below a velocity ratio of $R \approx 3.1$ and for the low density jet in crossflow[39] for a momentum flux ratio $J \lesssim 10$ or with a density ratio $S \lesssim 0.4$. These phenomena include: (1) clear changes in the spectral character of the shear-layer, with strong oscillations at narrow spectral peaks for global instability, representing pure tones with higher harmonics, as seen in Fig. 5(c); (2) a rather dramatic alteration in the value of the Strouhal number associated with the initial instability as the influencing flow parameter is brought into the range for globally unstable flow; (3) little spectral alteration of the globally unstable flow in response to low to moderate flow excitation, in contrast to significant spectral alteration of the convectively unstable flow during such excitation; (4) a rather abrupt increase in the amplitude of the disturbance within and near the shear-layer as one approaches the critical flow parameter, consistent with the characteristics of the forced Landau equation;[45,47] and (5) a reduction in the energy transfer from fundamental to subharmonic frequencies along the shear-layer, and hence a reduction in the strength of subharmonics and corresponding inhibition of the vortex pairing process after the transition.

For low density free jets, it is known that very strong external sinusoidal excitation can be used to overcome the fundamental instability mode for globally unstable conditions,[51,52] resulting in a "lock-in" to the applied forcing frequency f_f. A linear dependence of the critical amplitude above which lock-in occurs on $|f_f - f_0|$ is observed for the low density free jet by Juniper, Li, and Nichols,[52] suggesting a Hopf bifurcation to a global mode in their helium jet. Such lock-in behavior is also observed for both the equidensity transverse jet and the low density transverse jet. For example, Figure 6 shows this behavior for the low density tranvserse jet emanating from a flush nozzle[39] with jet-to-crossflow density ratio $S = 0.55$. This particular density ratio S is above the transition value for the low density free jet documented for this Reynolds number (1800 based on mean jet velocity); the jet-to-crossflow momentum flux ratio J needs to be less than approximately 10 to cause the shear layer to become globally unstable. Figure 6(a) shows the variation in response of the $J = 5$ jet shear layer for successively increasing jet forcing amplitudes at frequency f_f, which is greater than the natural, unforced shear layer frequency f_o. Here, the forcing amplitude is quantified in terms of the normalized pressure fluctuation p' created via the loudspeaker shown in Fig. 4. In the case shown, "lock-in" of the jet to f_f is achieved between normalized forcing amplitudes of 0.126 and 0.138. In a similar manner to the results of Juniper, Li, and Nichols,[52] many spectral peaks related to both f_o and f_f are observed at lower forcing amplitudes, as the competition between the natural and

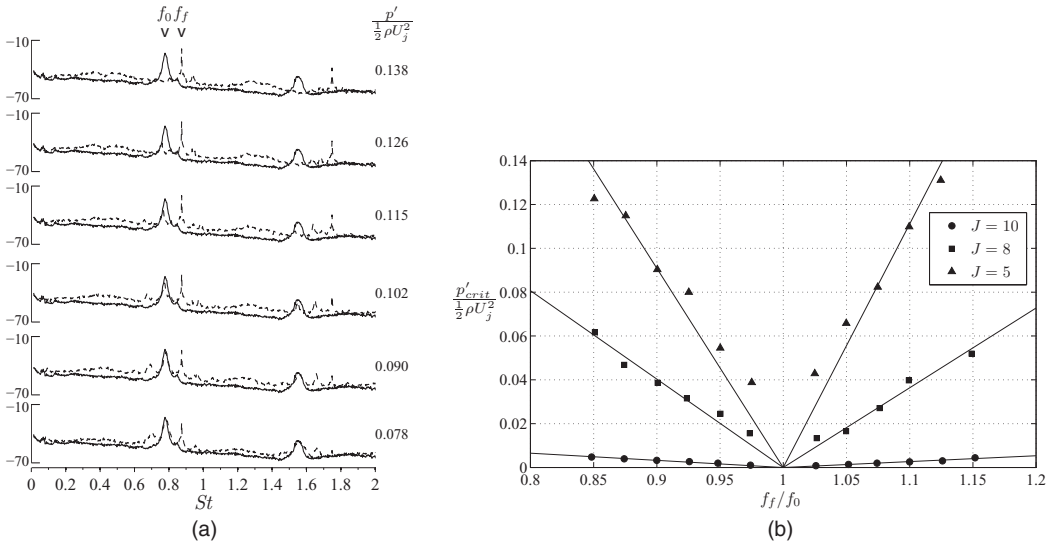

FIG. 6. (a) Power spectra (amplitude in dB) as measured at $s/D = 2.0$ in the transverse jet shear layer at several normalized forcing amplitudes for $J = 5$, $S = 0.55$, and $Re_j = 1800$. The dashed lines represent the spectra of the forced shear layer, and the solid lines represent the unforced shear layer spectra. Forcing is applied at $f_f = 2528$ Hz and the fundamental frequency is $f_0 = 2248$ Hz. (b) Forcing amplitude at which lock-in to the forcing frequency is achieved, as a function of forcing frequency f_f, for several values of J at density ratio $S = 0.55$. Reprinted with permission from D. R. Getsinger, C. Hendrickson, and A. R. Karagozian, Exp. Fluids **53**, 783–801 (2012). Copyright 2012 by Springer-Verlag.

imposed frequencies results in coupled nonlinear oscillator behavior. As shown in Figure 6(b), the dependence of the critical forcing amplitude for lock-in varies linearly with $|f_f - f_0|$, as is expected for an absolutely unstable flow. As J is increased to 8 and subsequently to 10 while maintaining $S = 0.55$, the same linear dependence is observed, but with the "V" shape opening up to allow effective lock-in of the shear layer at lower amplitudes of forcing. The global instability is clearly weakened as J is increased towards $J_{cr} \approx 10$, until even exceedingly low levels of forcing could be made effective in controlling the shear layer's oscillation frequency.

Results and trends for equidensity transverse jet shear layer stability in the convectively unstable range, i.e., for $R > 3.1$ for flush nozzle injection, are consistent with separate linear stability analyses by our group .[53,54] LSA with a continuous base flow representing the transverse jet itself[54] allows prediction of a maximum spatial growth rate for the disturbances. The nominally axisymmetric mode is found to be the most unstable mode in the transverse jet shear-layer's nearfield region, upstream of the end of the potential core. Maximum spatial growth rates and associated jet Strouhal numbers, St, extracted from this analysis both increase with decreasing velocity ratio R, in qualitative and quantitative agreement with the experimental results from Megerian *et al.*[37] in the range $4 < R \leq 10$. The comparisons between predicted and measured maxima in growth rates and Strouhal numbers are shown in Figures 7 and 8, respectively. The overall agreement of theoretical and experimental results confirms that convective instability occurs in the transverse jet shear-layer for these higher jet-to-crossflow velocity ratios, and that this instability is strengthened as R is decreased.

There have not been extensive theoretical examinations of transverse jet shear layer stability in the absolutely unstable regime. DNS and linear stability analysis of a pipe-generated transverse jet by Bagheri, *et al.*[55] suggest that the shear layer is globally linearly unstable at $R = 3$, although the pipe flow itself and detailed interactions between jet and crossflow at the exit plane of the jet are not represented. Recent direct numerical simulations (DNS) of the equidensity jet in crossflow by Mahesh and Iyer[56] do represent the presence of the flush nozzle, with flow and geometrical conditions identical to those in the experiments of Megerian *et al.*[37] For absolutely and convectively unstable conditions at velocity ratios $R = 2$ and 4, respectively, there is excellent qualitative and quantitative agreement between experiments and simulations in terms of velocity spectral characteristics.

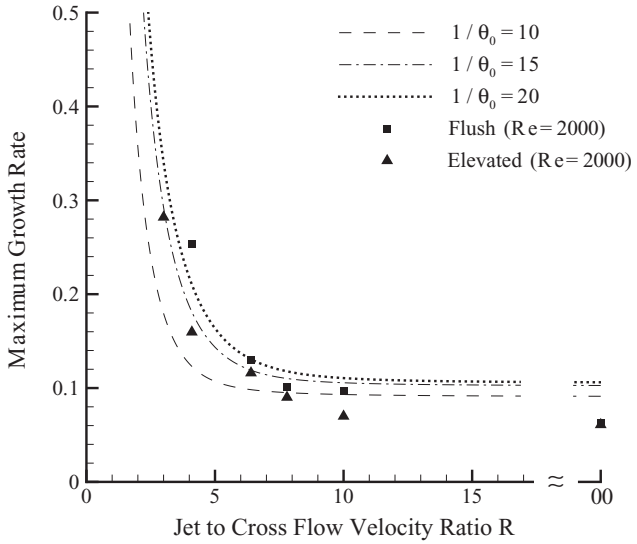

FIG. 7. Predicted growth rates associated with axisymmetric mode disturbances for the transverse jet upstream shear layer (from Alves, Kelly, and Karagozian[54]), with different lines corresponding to different values of θ_o, the local (initial) non-dimensional jet momentum thickness. The symbols represent experimentally measured values of initial growth rate (from Megerian *et al.*[37]), for different jet-to-crossflow velocity ratios $R \equiv 1/\lambda$ at a jet Reynolds number of 2000 (based on centerline jet velocity). Reprinted with permission from L. S. d. B. Alves, R. E. Kelly, and A. R. Karagozian, J. Fluid Mech. **602**, 383–401 (2008). Copyright 2008 by Cambridge University Press.

B. Implications of instabilities for jet excitation

The above-noted transition in shear layer stability characteristics, from convective instability at higher momentum flux or velocity ratios to absolute or global instability at low values of J or R, begins to explain the differences observed in our group's forced transverse jet studies[29,31] and

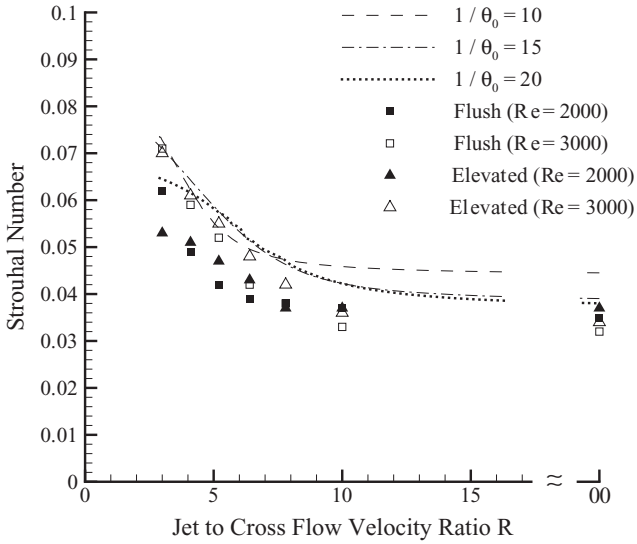

FIG. 8. Predicted Strouhal number associated with the most unstable axisymmetric mode disturbance from the LSA for the transverse jet (from Alves, Kelly, and Karagozian[54]), with different lines corresponding to different values of θ_o, the local (initial) non-dimensional jet momentum thickness. The symbols represent experimentally measured values of St (from Megerian *et al.*[37]) for different jet-to-crossflow velocity ratios $R \equiv 1/\lambda$ and at two different jet Reynolds numbers, 2000 and 3000 (based on centerline jet velocity), for both flush and elevated nozzles used in the experiments. Reprinted with permission from L. S. d. B. Alves, R. E. Kelly, and A. R. Karagozian, J. Fluid Mech. **602**, 383–401 (2008). Copyright 2008 by Cambridge University Press.

those of others.[30] The forced transverse jets studied in M'Closkey *et al.*[29] and Shapiro *et al.*[31] are at relatively low velocity ratios, 2.58 and 4.0 based on jet centerline velocity at the exit plane, and for a flush nozzle with nearly twice the exit diameter (7.5 mm) as in Megerian *et al.*[37] For the most part, these jets, and the shear layer spectral characteristics shown in Shapiro *et al.*,[31] exhibit absolutely unstable shear layer behavior, thus making it difficult to affect the jet via low-to-moderate amplitude sinusoidal excitation at forcing frequencies f_f that are not close to f_o. On the other hand, the transverse jets studied in Narayanan, Barooah, and Cohen,[30] at $R = 6$ and $Re_j = 5000$, are likely to have had convectively unstable shear layers, thus with greater susceptibility to influence by weak sinusoidal excitation. The observed response of the transverse jets to relatively weak sinusoidal excitation, that is, improved jet penetration and spread, is consistent with the behavior of a convectively unstable shear layer.

These shear layer instability characteristics not only explain these prior observations on jet excitation but also suggest that flow regime-dependent forcing strategies can be applied for the optimization and control of such jets in practical systems. For example, one can postulate that relatively low-level sinusoidal excitation could be employed to promote jet response and, potentially, enhanced mixing, when the transverse jet shear layer is experiencing convective instability, i.e., for higher momentum flux ratios as in dilution or fuel jet applications. But at lower values of J or R as in film cooling or similar applications, where the unforced JICF is likely to exhibit self-excited or absolutely unstable shear layer behavior, a different type of forcing is required to be able to affect penetration and spread.

This type of two-pronged strategy for excitation of the transverse jet has been explored by our group with respect to axisymmetric forcing of the jet fluid.[57] To enable exploration of temporal waveforms different from the standard sinusoidal excitation, we have used feedforward control, as used in prior jet excitation experiments,[29,31] but examining a rather wide range of equidensity flow conditions ($1.0 < R \leq 10.0$) and excitation conditions (forcing frequencies, amplitudes and, for square wave excitation, duty cycle or temporal pulsewidth). Sample results from these strategic forcing studies[57,58] are shown in Figs. 9 and 10. Smoke visualization for the transverse jet emanating from the elevated nozzle at a relatively high velocity ratio, $R = 10$, where the shear layer has been shown to be convectively unstable, demonstrates (Figs. 9(a)–9(c)) that sinusoidal excitation at a

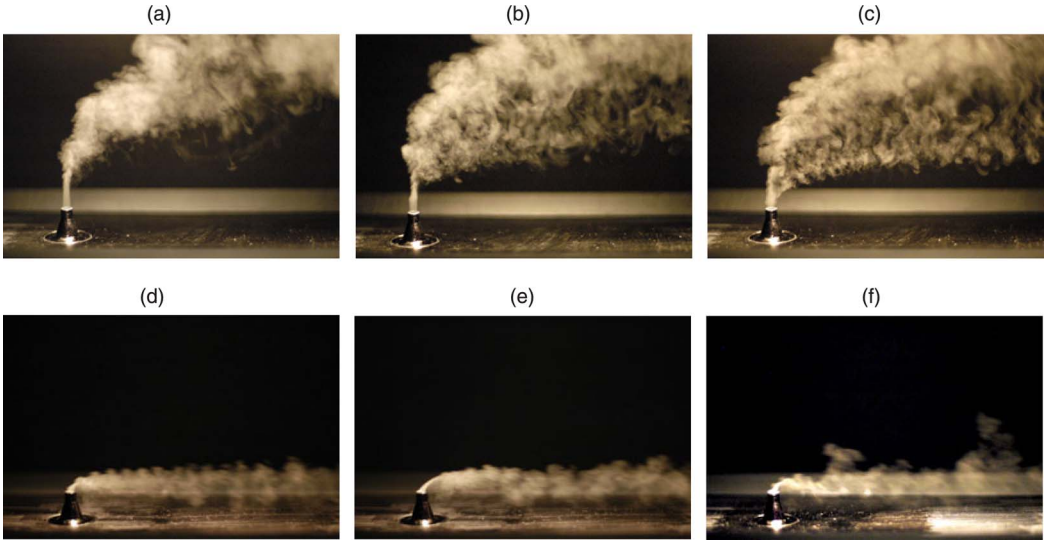

FIG. 9. Smoke visualization of the equidensity, elevated transverse jet with $R = 10$ and 1.15. Images are shown for jets with $R = 10$ and (a) no forcing, (b) sinusoidal forcing ($f_f = 0.10f_o = 147.2\ Hz$), and (c) square wave forcing ($f_f = 0.10f_o$) with $L/D = 4.9$, and for jets with $R = 1.15$ and (d) no forcing, (e) sinusoidal forcing ($f_f = 0.10f_o = 88\ Hz$), and (f) square wave forcing ($f_f = 0.10f_o$) with $L/D = 3.7$. $U'_{j,rms}$ was matched among corresponding forcing cases for each velocity ratio (1.7 m/s for $R = 10$ and 2.58 m/s for $R = 1.15$). Images are shown with an exposure time of 1/4000 s. Reprinted with permission from J. Davitian, C. Hendrickson, D. Getsinger, R. T. M'Closkey, and A. R. Karagozian, AIAA J. **48**, 2145–2156 (2010). Copyright 2010 by American Institute of Aeronautics and Astronautics, Inc.

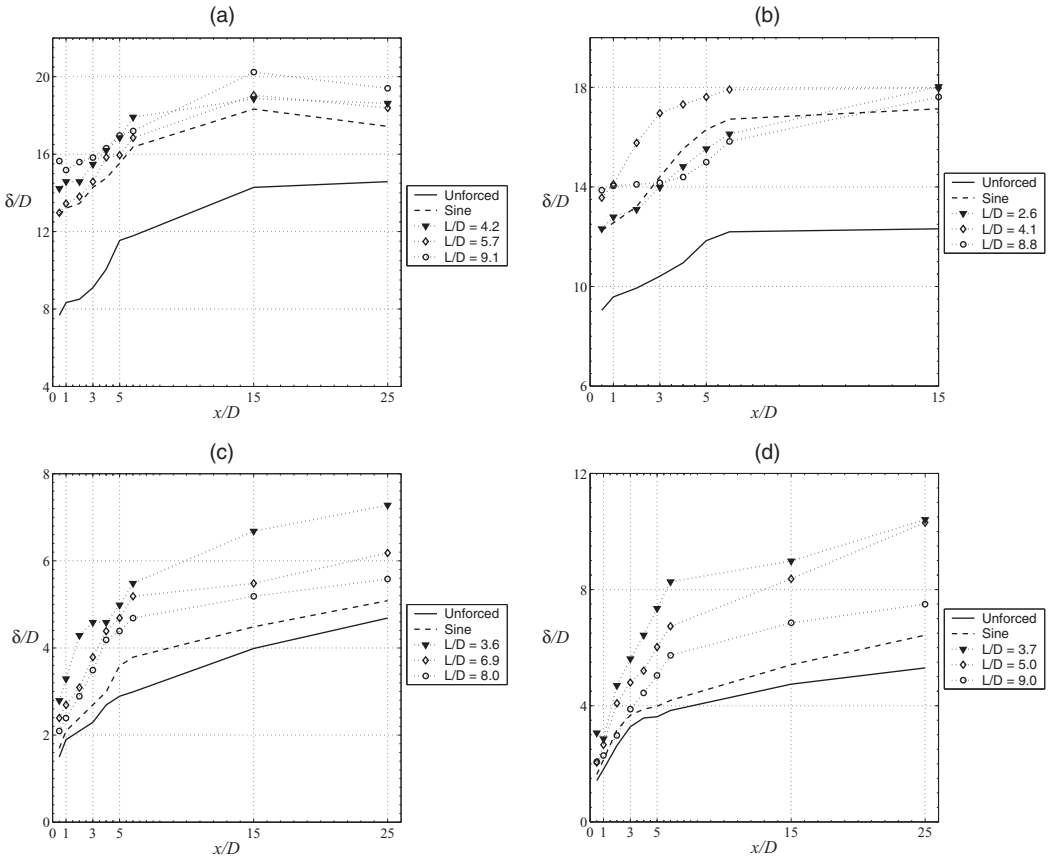

FIG. 10. Jet vertical spread quantification (δ/D) for $R = 10$ and $R = 1.15$ for the flush and elevated jets. (a) $R = 10$, flush nozzle. (b) $R = 10$, elevated nozzle. (c) $R = 1.15$, flush nozzle. (d) $R = 1.15$, elevated nozzle. Unforced cases are shown with solid lines, sinusoidal forcing with dashed lines, and square wave forcing results with corresponding L/D values are shown with symbols. Reprinted with permission from J. Davitian, C. Hendrickson, D. Getsinger, R. T. M'Closkey, and A. R. Karagozian, AIAA J. **48**, 2145–2156 (2010). Copyright 2010 by American Institute of Aeronautics and Astronautics, Inc.

moderate amplitude of excitation can improve jet spread nearly as well as can square wave excitation with the same effective amplitude, i.e., matched values of the RMS of the net velocity excitation at the jet's exit plane, $U'_{j,rms}$. This observed jet response, albeit via line-of-sight visualization, is quantified in measurements of jet spread, shown in Figs. 10(a) and 10(b) for both flush and elevated jets, respectively, at $R = 10$. Here it is clear that, for both cases where the shear layer is convectively unstable, sinusoidal excitation produces significantly greater jet spread (as well as penetration, quantified in Davitian *et al.*[57]) than that associated with the unforced JICF. In this figure, square wave excitation for optimized temporal pulsewidths is quantified in terms of an effective stroke ratio L/D, where L is determined by integrating measured jet centerline velocity at the exit plane over time. For $R = 10$, square wave forcing improves spread only slightly beyond that by sine wave forcing. On the other hand, when the transverse jet's shear layer is absolutely unstable in the absence of forcing, e.g., at $R = 1.15$ for either the elevated nozzle or flush nozzle, as shown in smoke visualization (Figs. 9(d)–9(f)) and spread quantification (Figs. 10(c) and 10(d)), moderate sinusoidal excitation has relatively little influence on jet response. On the other hand, square wave excitation at the same value of $U'_{j,rms}$, and with prescribed pulsewidths or stroke ratios L/D associated with optimal vortex ring formation,[34] can have a significant influence on jet response, as seen in these figures. It is noted that, despite the fact that transverse jet shear layer instabilities have only been quantified in the nearfield of the jet, developing and applying control strategies based on the state of the nearfield shear layer affects overall jet spread well into the farfield, at least to 25 diameters downstream of injection, as seen in both Figs. 9 and 10.

These and similar results in Davitian *et al.*[57] demonstrate the benefits of a physics-based strategy on the control of transverse jet behavior, which can be especially beneficial for specific application areas. More recent studies by our group have suggested further benefits from localized sensing within the jet actuation system to achieve closed loop control.[59,60] This new approach has been developed which adapts the controller parameters to the actuator dynamics (either a loudspeaker as shown in Fig. 4 or a modal shaker and piston arrangement). This approach yields the benefits of closed loop control with hotwire or microphone measurements or other sensing modalities, and is currently undergoing more extensive evaluation in our lab.

C. Transverse jet structural characteristics

As described above, understanding the transverse jet's upstream shear layer stability characteristics can provide a clear physical basis for developing strategies for jet control. While smoke visualization provides a useful means for capturing essential jet dynamics and for comparing jet penetration, spread, and structure under different excitation conditions, smoke imaging does not allow for a detailed quantitative study of shear layer characteristics, molecular mixing, or cross-sectional structure. Our group's recent and ongoing experimental studies of the low density and equidensity JICF use non-intrusive optical diagnostics for such quantification.[61–63] Planar laser-induced fluorescence (PLIF) imaging of acetone seeded in the jet and stereo particle image velocimetry (PIV) enable study of instantaneous and averaged jet behavior, including comparisons of unforced and forced jet structure under different flow conditions.

Details on the use of these experimental diagnostics for the transverse jet may be found in recent studies.[61–63] Acetone PLIF imaging in both the $x-z$ "centerplane" (at $y=0$) and $y-z$ cross-sectional planes (at various downstream locations x) reveal interesting relationships between jet structure and previously determined shear layer stability characteristics. For example, when the jet-to-crossflow velocity ratio or momentum flux ratio for the flush nozzle is relatively high, corresponding to convectively unstable shear layer conditions (e.g., $J > 10$), the relatively weak instability in the shear layer is quite visible, with delayed rollup in the shear layer vorticity. In contrast, there is rapid nearfield rollup of shear layer vortex structures for absolutely unstable shear layer conditions ($J < 10$). Examples of these differences in shear layer structure for the equidensity JICF are shown in Figs. 11(a) and 11(b), contrasting instantaneous acetone PLIF centerplane images for $J = 30$ and $J = 5$, respectively. More unexpected are the ensemble-averaged acetone PLIF concentration fields obtained for cross-sectional slices of the flush nozzle-generated JICF at a fixed downstream location. Cross-sectional slices of the jet at $x/D = 10.5$ downstream of injection, shown in Figs. 11(c) and 11(d) for $J = 30$ and $J = 5$, respectively, represent images averaged over 300 instantaneous flowfield snapshots. The absolutely unstable transverse jet at $J = 5$, with rapid upstream shear layer rollup, produces a mean cross-section which takes on the counter-rotating vortex pair structure typically associated with the JICF. But at the higher momentum flux ratio, $J = 30$, the mean cross-section is not the symmetric CVP but rather a skewed structure that also shows evidence of a "tertiary" vortical structure below the mean jet, similar to that seen in Kuzo[65] and Shan and Dimotakis[66] at high jet-to-crossflow velocity ratios ($R \geq 10$) and jet Reynolds numbers in the same regime as those explored by our group. As documented in detail for other flow conditions,[63,64] this kind of asymmetric cross-section is observed for higher J values (above approximately 20) and for jet Reynolds numbers below approximately 4000, although slight asymmetries are still observed for Re_j as high as 6500, suggesting that a more thorough examination of transverse jet shear layer stability characteristics at high Reynolds numbers would be useful. Small asymmetries in jet cross-sections at $Re_j = 6000$ are also observed by Narayanan, Barooah, and Cohen[30] and Muldoon and Acharya[32] for $R = 6$ and $Re_j = 6000$, and by Smith and Mungal[14] at $R = 10$ and 20 (for $Re_j = 16\,000$ and 33 000, respectively). Our experiments suggest that the strongest predictor of transverse jet cross-sectional symmetry is in fact the proximity of shear layer rollup to the jet injection plane, as postulated by Kelso, Lim, and Perry,[7] which occurs most commonly for flush jet injection under absolutely unstable shear layer conditions. Transverse jet structural characteristics for the elevated nozzle as well as a straight flush

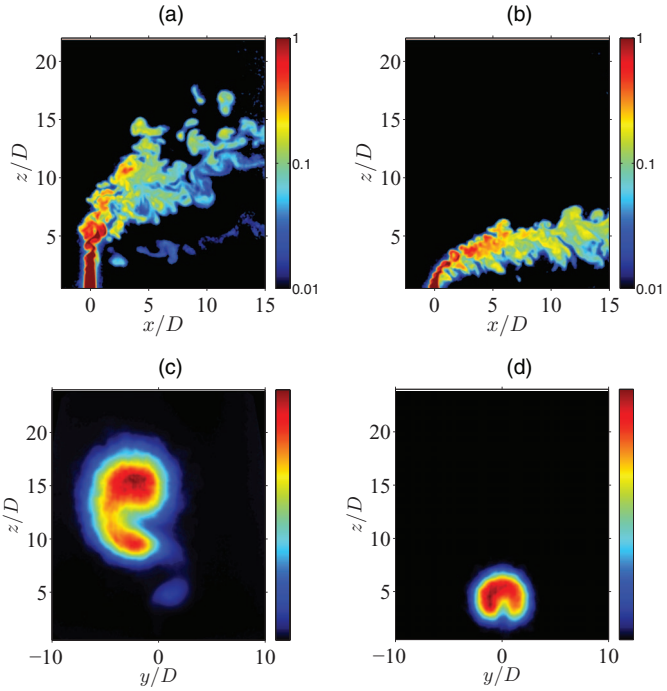

FIG. 11. Centerplane (side) instantaneous acetone PLIF imaging of the flush nozzle-generated JICF with $Re_j = 1900$ and density ratio $S = 1.0$ for (a) $J = 30$ and (b) $J = 5$. Cross-sectional jet slices at $x/D = 10.5$, averaged over 300 images, for the same flush nozzle and flow conditions, for (c) $J = 30$ and (d) $J = 5$. (Courtesy: L. Gevorkyan, private communication, 2014). (a) $J = 30$, centerplane. (b) $J = 5$, centerplane. (c) $J = 30$, cross-section. (d) $J = 5$, cross-section.

pipe-injected jet are also described in these recent studies,[63] for equidensity as well as low density jet conditions.

III. CONCLUSIONS AND OUTSTANDING ISSUES

There are a number of outstanding questions that emerge from these studies on shear layer stability and structural characteristics for equidensity and low density jets in crossflow. Non-intrusive diagnostics not only enable exploration of transverse jet structural characteristics, as shown in Fig. 11, but centerplane-based as well as cross-section-based mixing characteristics may also be extracted. A fundamental question naturally follows the stability studies: Is the absolutely unstable JICF better mixed than the convectively unstable JICF, as is often the case for self-excited flows?[40] PLIF-based mixing metrics that may be extracted to help to answer this question include centerline concentration decay and spread, as studied for transverse jets at higher Reynolds numbers by Smith and Mungal,[14] but also can include quantification of molecular unmixedness,[67] determination of probability density function for the concentration field,[68] and metrics relevant to reactive flows, such as scalar dissipation rates,[69] for both centerplane and cross-sectional images of the transverse jet.

These mixing metrics may be significantly different from one another based on JICF flow conditions. The unexpected features of the JICF in terms of structural asymmetries and the possible linkage of structure to the state of the jet's shear layer, vorticity rollup, and thus to the degree of molecular mixing, introduce a host of additional fundamental issues and questions. Does the state of the shear layer always predict whether or not the CVP will form, and whether or not the structure will be symmetric? Why is symmetry seemingly difficult to achieve in the convectively unstable regime, as suggested by Smith and Mungal[14] and studied more recently by our group?[63] While the (supposedly symmetric) CVP has long been thought to be responsible for the transverse jet's ability to improve mixing with the surroundings in comparison to the free jet,[4] do the state of the shear layer and flow asymmetries affect the nature of molecular mixing itself, and if so, how? The

smoke-visualized, line-of-sight jet spread measurements indicated in Fig. 10 do not tell the whole story with respect to local and global mixing, but neither do PLIF-based centerplane jet images (e.g., Figs. 11(a) and 11(b)) and the associated concentration decay, given that different flow conditions create both symmetric and asymmetric jet cross-sections that do not enable complete characterization of jet entrainment via the centerplane. Hence not only are cross-sectional metrics important to consider, but there are additional questions on the fundamental nature of mixing and how it could or should be quantified for this complicated, temporally variable three-dimensional flowfield, even in the absence of external forcing. Ultimately, in order for the control of this flowfield to be possible in realistic engineering systems, where upsets in operating conditions can alter the state of the flow and hence the structure and means by which it needs to be controlled, these open questions should be addressed.

ACKNOWLEDGMENTS

The author wishes to express her profound thanks to a number of faculty colleagues and present and former students who have been instrumental to much of the research described herein as well as her understanding of and appreciation for this remarkable flowfield. These individuals include Professor Luca Cortelezzi of McGill University; Professors Robert M'Closkey, Owen Smith, and Robert Kelly of UCLA; former graduate students Jonathan King, Stephen Shapiro, Sevan Megerian, Marcus George, Leonardo Alves, Juliett Davitian, Kevin Canzonieri, Daniel Getsinger, and Cory Hendrickson; present graduate students Levon Gevorkyan and Takeshi Shoji; and a host of undergraduate research assistants. Financial support for this research by the National Science Foundation under Grant Nos. CBET-0755104 and CBET-1133015, the Air Force Office of Scientific Research under Grant No. FA9550-11-1-0128, and the NASA Graduate Student Researchers Program is gratefully acknowledged.

[1] R. J. Margason, "Fifty years of jet in cross flow research," in *Proceedings of the AGARD Symposium on Computational and Experimental Assessment of Jets in Crossflow, AGARD-CP-534 (Advisory Group for Aerospace Research and Development), London* (North American Treaty Organization (NATO), 1993), pp. 1–141, Vol. 1.
[2] A. R. Karagozian, "Transverse jets and their control," Prog. Energy Combus. Sci. **36**, 531–553 (2010).
[3] Y. Kamotani and I. Greber, "Experiments on a turbulent jet in a cross flow," AIAA J. **10**, 1425–1429 (1972).
[4] R. Fearn and R. Weston, "Vorticity associated with a jet in a crossflow," AIAA J. **12**, 1666–1671 (1974).
[5] Z. M. Moussa, J. W. Trischka, and S. Eskinazi, "The nearfield in the mixing of a round jet with a cross-stream," J. Fluid Mech. **80**, 49–80 (1977).
[6] J. Andreopoulos, "On the structure of jets in a crossflow," J. Fluid Mech. **157**, 163–197 (1985).
[7] R. M. Kelso, T. T. Lim, and A. E. Perry, "An experimental study of round jets in cross-flow," J. Fluid Mech. **306**, 111–144 (1996).
[8] L. Cortelezzi and A. R. Karagozian, "On the formation of the counter-rotating vortex pair in transverse jets," J. Fluid Mech. **446**, 347–373 (2001); available at http://journals.cambridge.org/action/displayAbstract?fromPage=online&aid=87833&fulltextType=RA&fileId=S0022112001005894.
[9] S. Muppidi and K. Mahesh, "Direct numerical simulation of round turbulent jets in crossflow," J. Fluid Mech. **574**, 59–84 (2007).
[10] K. Mahesh, "The interaction of jets with crossflow," Annu. Rev. Fluid Mech. **45**, 379–407 (2013).
[11] A. Krothapalli, L. Lourenco, and J. M. Buchlin, "Separated flow upstream of a jet in a crossflow," AIAA J. **28**, 414–420 (1990).
[12] R. M. Kelso and A. J. Smits, "Horseshoe vortex systems resulting from the interaction between a laminar boundary layer and a transverse jet," Phys. Fluids **7**, 153–158 (1995).
[13] T. F. Fric and A. Roshko, "Vortical structure in the wake of a transverse jet," J. Fluid Mech. **279**, 1–47 (1994).
[14] S. H. Smith and M. G. Mungal, "Mixing, structure and scaling of the jet in crossflow," J. Fluid Mech. **357**, 83–122 (1998).
[15] J. D. Holdeman, "Mixing of multiple jets in a confined subsonic crossflow," Prog. Energy Comb. Sci. **19**, 31–70 (1993).
[16] J. P. Bons, R. Sondergaard, and R. B. Rivir, "The fluid dynamics of lpt blade separation control using pulsed jets," J. Turbomach. **124**, 77–85 (2002).
[17] S. V. Ekkad, S. Ou, and R. B. Rivir, "Effect of jet pulsation and duty cycle on film cooling from a single jet on a leading edge model," J. Turbomach. **128**, 564–571 (2006).
[18] J. E. Broadwell and R. E. Breidenthal, "Structure and mixing of a transverse jet in incompressible flow," J. Fluid Mech. **148**, 405–412 (1984).
[19] A. R. Karagozian, "An analytical model for the vorticity associated with a transverse jet," AIAA J. **24**, 429–436 (1986).
[20] A. R. Karagozian, "The flame structure and vorticity generated by a chemically reacting transverse jet," AIAA J. **24**, 1502–1507 (1986).
[21] T. A. Brzustowski, "Hydrocarbon turbulent diffusion flame in subsonic crossflow," *Turbulent Combustion*, Progress in Astronautics and Aeronautics Vol. 58 (AIAA (American Institute of Aeronautics and Astronautics), 1977), pp. 407–430.

[22] J. S. Abbitt, C. Segal, J. C. McDaniel, R. H. Krauss, and R. B. Whitehurst, "Experimental supersonic hydrogen combustion employing staged injection behind a rearward-facing step," J. Propul. Power **9**, 472–478 (1993).
[23] K. S. C. Wang, O. I. Smith, and A. R. Karagozian, "In-flight imaging of gas jets injected into subsonic and supersonic crossflows," AIAA J. **33**(12), 2259–2263 (1995).
[24] A. R. Karagozian, K. S. C. Wang, A.-T. Le, and O. I. Smith, "Transverse gas jet injection behind a rearward-facing step," J. Propul. Power **12**(6), 1129–1136 (1996).
[25] E. T. Curran, "Scramjet engines: The first forty years," J. Propul. Power **17**, 1138–1148 (2001).
[26] P. J. Vermeulen, P. Grabinski, and V. Ramesh, "Mixing of an acoustically excited air jet with a confined hot crossflow," ASME Trans. J. Eng. Gas Turbines Power **114**, 46–54 (1992).
[27] H. Johari, M. Pacheco-Tougas, and J. C. Hermanson, "Penetration and mixing of fully modulated turbulent jets in crossflow," AIAA J. **37**, 842–850 (1999).
[28] A. Eroglu and R. E. Breidenthal, "Structure, penetration, and mixing of pulsed jets in crossflow," AIAA J. **39**, 417–423 (2001).
[29] R. T. M'Closkey, J. King, L. Cortelezzi, and A. R. Karagozian, "The actively controlled jet in crossflow," J. Fluid Mech. **452**, 325–335 (2002).
[30] S. Narayanan, P. Barooah, and J. M. Cohen, "Dynamics and control of an isolated jet in crossflow," AIAA J. **41**, 2316–2330 (2003).
[31] S. Shapiro, J. King, R. T. M'Closkey, and A. R. Karagozian, "Optimization of controlled jets in crossflow," AIAA J. **44**, 1292–1298 (2006).
[32] F. Muldoon and S. Acharya, "Direct numerical simulation of pulsed jets in crossflow," Comput. Fluids **39**, 1745–1773 (2010).
[33] L. Cortelezzi, R. T. M'Closkey, and A. R. Karagozian, "A framework to design controllers for engineering applications of transverse jets," in *Manipulation and Control of Transverse Jets*, CISM Courses and Lectures No. 439, edited by A. Karagozian, L. Cortelezzi, and A. Soldati (Springer–Wein, New York, 2003).
[34] M. Gharib, E. Rambod, and K. Shariff, "A universal time scale for vortex ring formation," J. Fluid Mech. **360**, 121–141 (1998).
[35] H. Johari, "Scaling of fully pulsed jets in crossflow," AIAA J. **44**, 2719–2725 (2006).
[36] R. Sau and K. Mahesh, "Optimization of pulsed jets in crossflow," J. Fluid Mech. **653**, 365–390 (2010).
[37] S. Megerian, J. Davitian, L. S. de B. Alves, and A. R. Karagozian, "Transverse-jet shear-layer instabilities. Part 1. Experimental studies," J. Fluid Mech. **593**, 93–129 (2007).
[38] J. Davitian, D. Getsinger, C. Hendrickson, and A. R. Karagozian, "Transition to global instability in transverse-jet shear layers," J. Fluid Mech. **661**, 294–315 (2010).
[39] D. R. Getsinger, C. Hendrickson, and A. R. Karagozian, "Shear layer instabilities in low-density transverse jets," Exp. Fluids **53**, 783–801 (2012).
[40] P. A. Monkewitz, D. W. Bechert, B. Barsikow, and B. Lehmann, "Self-excited oscillations and mixing in a heated round jet," J. Fluid Mech. **213**, 611–639 (1990).
[41] R. A. Petersen and M. M. Samet, "On the preferred mode of jet instability," J. Fluid Mech. **194**, 153–173 (1988).
[42] G. Xu and R. A. Antonia, "Effect of different initial conditions on a turbulent round free jet," Exp. Fluids **33**, 677–683 (2002).
[43] A. K. M. F. Hussain and K. B. M. Q. Zaman, "The free shear layer tone phenomenon and probe interference," J. Fluid Mech. **87**, 349–383 (1978).
[44] S. Jendoubi and P. J. Strykowski, "Absolute and convective instability of axisymmetric jets with external flow," Phys. Fluids **6**, 3000–3009 (1994).
[45] P. Huerre and P. A. Monkewitz, "Local and global instabilities in spatially developing flows," Annu. Rev. Fluid Mech. **22**, 473–537 (1990).
[46] D. M. Kyle and K. R. Sreenivasan, "The instability and breakdown of a round variable-density jet," J. Fluid Mech. **249**, 619–664 (1993).
[47] P. J. Strykowski and D. L. Niccum, "The stability of countercurrent mixing layers in circular jets," J. Fluid Mech. **227**, 309–343 (1991).
[48] P. J. Strykowski and D. L. Niccum, "The influence of velocity and density ratio on the dynamics of spatially developing mixing layers," Phys. Fluids A **4**, 770–781 (1992).
[49] M. Provansal, C. Mathis, and L. Boyer, "Benard-von karman instability: Transient and forced regimes," J. Fluid Mech. **182**, 1–22 (1987).
[50] D. Hammond and L. Redekopp, "Global dynamics of symmetric and asymmetric wakes," J. Fluid Mech. **331**, 231–260 (1997).
[51] M. P. Hallberg and P. J. Strykowski, "Open-loop control of fully nonlinear self-excited oscillations," Phys. Fluids **20**, 041703 (2008).
[52] M. P. Juniper, L. K. B. Li, and J. W. Nichols, "Forcing of self-excited round jet diffusion flames," Proc. Combus. Inst. **32**, 1191–1198 (2009).
[53] L. S. d. B. Alves, R. E. Kelly, and A. R. Karagozian, "Local stability analysis of an inviscid transverse jet," J. Fluid Mech. **581**, 401–418 (2007).
[54] L. S. d. B. Alves, R. E. Kelly, and A. R. Karagozian, "Transverse-jet shear-layer instabilities. Part 2. Linear analysis for large jet-to-crossflow velocity ratio," J. Fluid Mech. **602**, 383–401 (2008).
[55] S. Bagheri, P. Schlatter, P. J. Schmid, and D. S. Henningson, "Global stability of a jet in crossflow," J. Fluid Mech. **624**, 33–44 (2009).
[56] K. Mahesh and P. Iyer, "Numerical study of shear layer instability in transverse jets," Bull. Am. Phys. Soc. **58**(18), 174 (2013).

[57] J. Davitian, C. Hendrickson, D. Getsinger, R. T. M'Closkey, and A. R. Karagozian, "Strategic control of transverse jet shear layer instabilities," AIAA J. **48**, 2145–2156 (2010).
[58] J. Davitian, "Exploration and controlled excitation of transverse jet shear layer instabilities," Ph.D. thesis (University of California, Los Angeles, Department of Mechanical and Aerospace Engineering, 2008).
[59] C. Hendrickson and R. M'Closkey, "Phase compensation strategies for modulated-demodulated control with application to pulsed jet injection," ASME J. Dyn. Syst., Measur., Control **134**, 011024-1–011024-9 (2012).
[60] C. S. Hendrickson, "Identification and control of the jet in crossflow," Ph.D. thesis (University of California, Los Angeles, Department of Mechanical and Aerospace Engineering, 2012).
[61] D. Getsinger, "Shear layer instabilities and mixing in variable density transverse jet flows," Ph.D. thesis (UCLA, 2012).
[62] D. Getsinger, L. Gevorkyan, C. Hendrickson, O. I. Smith, and A. R. Karagozian, "Scalar and velocity field measurements in acoustically excited variable density transverse jets," AIAA Paper No. 2012-1225, 2012.
[63] L. Gevorkyan, D. Getsinger, O. I. Smith, and A. R. Karagozian, "Structural and stability characteristics of jets in crossflow," AIAA Paper No. 2014-0230, 2014.
[64] L. Gevorkyan, private communication (2014).
[65] D. M. Kuzo, "An experimental study of the turbulent transverse jet," Ph.D. thesis (California Institute of Technology, 1995).
[66] J. Shan and P. Dimotakis, "Reynolds-number effects and anisotropy in transverse-jet mixing," J. Fluid Mech. **566**, 47–96 (2006).
[67] P. Danckwerts, "The definition and measurement of some characteristics of mixtures," Appl. Sci. Res. **A3**, 279–296 (1952).
[68] P. Dimotakis, "The mixing transition in turbulent flows," J. Fluid Mech. **409**, 69–98 (2000).
[69] E. S. Bish and W. J. A. Dahm, "Strained dissipation and reaction layer analyses of nonequilibrium chemistry in turbulent reacting flows," Combus. Flame **100**, 457–464 (1994).